

Thiol Oxidation Causes Pulmonary Vasodilation by Activating K⁺ Channels and Inhibiting Store-operated Ca²⁺ Channels

Christian Schach, Minlin Xu, Oleksandr Platoshyn, Steve H. Keller, and Jason X.-J. Yuan[†]

Division of Pulmonary and Critical Care Medicine, Department of Medicine, University of California, San Diego, La Jolla, California 92093-0725

Running title: Diamide inhibits pulmonary vasoconstriction

[†]Correspondence and reprint request should be addressed to:

Jason X.-J. Yuan, M.D., Ph.D.
Division of Pulmonary and Critical Care Medicine
Medical Teaching Facility, Rm. 252
University of California, San Diego
9500 Gilman Drive, MC 0725
La Jolla, CA 92093-0725

Tel: (858) 822-6534
Fax: (858) 822-6531
E-mail: xiyuan@ucsd.edu

Abstract

Cellular redox change regulates pulmonary vascular tone by affecting function of membrane and cytoplasmic proteins, enzymes and second messengers. This study was designed to test the hypothesis that functional modulation of ion channels by thiol oxidation contributes to regulating excitation-contraction coupling in isolated pulmonary artery (PA) rings. Acute treatment with the thiol oxidant diamide produced a dose-dependent relaxation in PA rings; the IC₅₀ was 335 and 58 μM for 40 mM K⁺- and 2 μM phenylephrine (PE)-induced PA contraction, respectively. The diamide-mediated pulmonary vasodilation was neither affected by functional removal of endothelium nor by 8-Br-cGMP (50 μM) and HA-1004 (30 μM). A rise in extracellular [K⁺] (from 20 to 80 mM) attenuated the thiol oxidant-induced PA relaxation. Passive store depletion by cyclopiazonic acid (CPA, 50 μM) and active store depletion by PE (in the absence of external Ca²⁺) both induced PA contraction due to capacitative Ca²⁺ entry (CCE). Thiol oxidation by diamide significantly attenuated CCE-induced PA contraction due to active and passive store depletion. The PA rings isolated from left and right PA branches appeared to respond differently to store depletion. While the active tension induced by passive store depletion was comparable, the active tension induced by active store depletion was 3.5-fold greater in right branches than in left branches. These data indicate that thiol oxidation causes pulmonary vasodilation by activating K⁺ channels and inhibiting store-operated Ca²⁺ channels, which subsequently attenuate Ca²⁺ influx and decrease [Ca²⁺]_{cyt} in pulmonary artery smooth muscle cells. The mechanisms involved in thiol oxidation-mediated pulmonary vasodilation or activation of K⁺ channels and inhibition of store-operated Ca²⁺ channels appear to be independent of functional endothelium and of the cGMP-PKG pathway.

Key words: diamide; pulmonary artery; smooth muscle contractility; pulmonary hypertension; capacitative calcium entry; redox status

Introduction

The pulmonary circulation system is a low pressure and low resistance system that receives the whole cardiac output. Pulmonary vascular smooth muscle contractility is mainly controlled by the level of cytosolic free Ca^{2+} ($[\text{Ca}^{2+}]_{\text{cyt}}$) in pulmonary artery smooth muscle cells (PASMC) (23, 54, 82) and modulated by circulating vasoactive substances, and by vasoconstrictive and vasodilatative factors derived from endothelial cells (9, 27, 43, 75). Sustained pulmonary vasoconstriction is an important cause for the elevated pulmonary vascular resistance in animals with hypoxia-induced pulmonary hypertension and in patients with idiopathic pulmonary arterial hypertension (50, 56). Persistent pulmonary vasoconstriction is also involved in initiating pulmonary vascular remodeling by stimulating PASMC proliferation and hypertrophy (79).

One of the unique properties of the pulmonary vasculature is the vasoconstrictive response to acute and chronic alveolar hypoxia, which is opposite to the vasodilating response of systemic vessels to hypoxia and ischemia (37, 44, 68, 81). Although the cellular and molecular mechanisms involved in hypoxic pulmonary vasoconstriction remain unclear, the redox status change in pulmonary vascular smooth muscle and endothelial cells has been implicated in regulating pulmonary vascular tone via modulating $[\text{Ca}^{2+}]_{\text{cyt}}$ in PASMC (64, 71). Hypoxia may have multiple effects on cellular redox status depending on the basal status of PASMC, participating regulators and effectors in PASMC (e.g., different ion channels and receptors in the plasma membrane, capacity of intracellular Ca^{2+} stores) and interaction between smooth muscle cells and endothelial cells (1, 32).

Experiments *in vitro* and *in vivo* using isolated pulmonary arteries, isolated perfused lungs and intact animals have well demonstrated that an increase in $[\text{Ca}^{2+}]_{\text{cyt}}$ in PASMC is a

major trigger for smooth muscle contraction and pulmonary vasoconstriction (11, 40, 67). Inhibition of Ca^{2+} influx with Ca^{2+} channel blockers (e.g., nifedipine, verapamil) improves hemodynamics in patients with pulmonary hypertension (55, 66, 72). When $[\text{Ca}^{2+}]_{\text{cyt}}$ rises in PASMC, Ca^{2+} binds to calmodulin, which activates myosin light chain kinase to phosphorylate the myosin light chain. This phosphorylation increases the activity of myosin ATPase that hydrolyzes ATP, thereby releasing energy. The subsequent cycling of the myosin cross-bridges produces displacement of the myosin filament in relation to the actin filament causing contraction (61). The excitation-contraction coupling in vascular smooth muscle takes place through two major mechanisms: *i*) electromechanical coupling, the mechanism that causes contraction or relaxation through changes in membrane potential (E_m), and *ii*) pharmacomechanical coupling, the complex of mechanisms that can cause contraction or relaxation by mechanisms not mediated by changes in E_m (21, 62).

PASMC express multiple Ca^{2+} channels that open in response to electrical and pharmacological stimulation to increase $[\text{Ca}^{2+}]_{\text{cyt}}$. There are at least three functionally distinct Ca^{2+} channels in PASMC (25, 45): *a*) voltage-dependent Ca^{2+} channels (VDCC) that are activated by membrane depolarization (e.g., by raising extracellular K^+ or inhibiting K^+ channel activity), *b*) receptor-operated Ca^{2+} channels (ROC) that are opened by agonist- or mitogen-mediated receptor activation and synthesis of phospholipase and diacylglycerol, and *c*) store-operated Ca^{2+} channels (SOC) that are opened by active and passive depletion of intracellular Ca^{2+} stores, such as the sarcoplasmic or endoplasmic reticulum.

This study was designed to investigate whether oxidation of pulmonary vascular smooth muscle and endothelial cells by the thiol oxidant diamide affects electromechanical and

(LCMP-00276-2006.R2) 5

pharmacomechanical coupling in isolated pulmonary arteries and what mechanisms are potentially involved in the thiol oxidant-mediated regulation of pulmonary vascular tone.

Materials and Methods

Isolation of pulmonary arterial rings and tension measurement. The right and left branches (2nd division) of the main pulmonary artery (PA) as well as the intrapulmonary arteries (3rd and 4th division) were isolated from male Sprague-Dawley rats (100-250 g). The adipose, connective tissues and adventitia were carefully removed, and the remaining muscular arteries were cut into 2 mm-long rings. For some of the experiments, the endothelium of PA rings was removed by gently rubbing the inner lumen of the vessels with a rough wooden stick. Functional removal of the endothelium was confirmed by the loss of relaxant response of PA rings to acetylcholine (ACh, 10 µM). This procedure did not damage the vessels because phenylephrine (PE)- or high K⁺-mediated active tension was actually enhanced in PA rings with denuded endothelium.

Two stainless steel hooks (0.1 mm in diameter) were inserted through the lumen of PA rings. One hook was mounted in a perfusion chamber (1 ml in volume) and the other hook was connected to an isometric force transducer (Harvard Apparatus). Isometric tension was continuously monitored and recorded using DATAQ data acquisition software (DATAQ Instruments). Resting passive tension, i.e., that offering maximal tension in rings exposed to 40 mM K⁺ (40K), was 600 mg. The rings were equilibrated for 1 hr at resting (or basal) tension, and then challenged three times with 40K-perfusate to obtain a stable contractile response. After experiments, each PA ring was weighed using a fine balance. The active tension (mg) was normalized by wet tissue weight (mg) and expressed in milligram tension per milligram weight (mg/mg).

Isolated PA rings were superfused with modified Krebs solution (MKS) consisting of 138 mM NaCl, 1.8 mM CaCl₂, 4.7 mM KCl, 1.2 mM MgSO₄, 1.2 mM NaH₂PO₄, 5 mM HEPES, and 10 mM glucose (pH 7.4, at 37°C). In Ca²⁺-free (0Ca) solution, CaCl₂ was replaced by equimolar

(LCMP-00276-2006.R2) 7

MgCl₂ and 1 mM EGTA was added to chelate residual Ca²⁺. In the high-K⁺ solution, NaCl was replaced by equimolar KCl to maintain osmolarity.

Cell preparation and culture. Rat pulmonary artery smooth muscle cells (PASMC) were prepared from pulmonary arteries of male Sprague-Dawley rats. Briefly, the isolated pulmonary arteries were incubated for 20 min in Hanks' balanced salt solution (HBSS) containing 1.5 mg/ml collagenase (Worthington Biochemical, Lakewood, NJ). Adventitia and endothelium were carefully removed after the incubation. The remaining smooth muscle was digested for 45-50 min with 1.5-mg/ml collagenase and 0.5 mg/ml elastase (Sigma, St. Louis, MO) at 37°C. PASMC were sedimented by centrifugation, resuspended in fresh media, and plated. In addition, the embryonic rat heart-derived myogenic cell line H9c2 (12), purchased from the American Type Culture Collection, was used for some experiments. The H9c2 cells were cultured in Dulbecco's modified Eagle's medium (DMEM) containing 10% fetal bovine serum (FBS). Subconfluent H9c2 cells were then plated onto cover slips and cultured in 10% FBS-DMEM for 3-5 days before patch clamp experiments.

Electrophysiological measurements. Whole-cell K⁺ currents were recorded at room temperature (22-24°C) from PASMC using an Axopatch 1D amplifier and a DigiData 1200 interface (Axon Instruments; Union City, CA). Cells were plated on glass cover slips, mounted on a plastic glass cell-perfusion chamber on a Nikon inverted microscope, and bathed in physiological saline solution (PSS). Borosilicate patch pipettes (2-4 MΩ) were fabricated on a Model P-97 electrode puller (Sutter Instruments; Novato, CA) and polished with a MF-63 microforge (Narashige Scientific Instruments Laboratories; Tokyo, Japan). Step-pulse protocols and data acquisition

were performed using pCLAMP software. Currents were filtered at 1-2 kHz (-3 dB) and digitized at 2-4 kHz. Series resistance compensation was performed in all whole-cell experiments. Leak and capacitative currents were subtracted using the P/4 protocol in pCLAMP software.

For recording optimal whole-cell K_v currents ($I_{K(V)}$), cells were superfused with a standard extracellular solution containing 141 mM NaCl, 4.7 mM KCl, 3.0 mM MgCl₂, 10 mM HEPES, 1 mM EGTA, and 10 mM glucose (pH 7.4). The pipette (intracellular) solution contained 135 mM KCl, 4 mM MgCl₂, 10 mM HEPES, 10 mM EGTA, and 5 mM Na₂ATP (pH 7.2). Under these conditions, the contribution of ATP-sensitive (K_{ATP}) K⁺ channels and Ca²⁺-activated (K_{Ca}) K⁺ channels to the whole-cell currents was minimized because of high concentrations of ATP (5 mM) and EGTA (10 mM) in the pipette (intracellular) solution.

Solutions and chemicals. Cyclopiazonic acid (CPA, Sigma), nifedipine (Sigma), and diamide (Sigma) were dissolved in DMSO to make stock solutions of 50, 100, and 500 mM, respectively; aliquots of the stock solutions were then diluted in MKS or Ca²⁺-free MKS on the day of use to their final concentrations. Acetylcholine (ACh, Sigma), 8-bromoguanosine-3'-5'-cyclomonophosphate (8-Br-cGMP, Fluka), cromakalim (Sigma), N-(2-guanidinoethyl)-5-isoquinolinesulfonamide hydrochloride (HA-1004, Sigma), DL-dithiothreitol (DTT), 4-aminopyridine (4-AP, Sigma), hydrogen peroxide (H₂O₂, Sigma), and phenylephrine (PE, Sigma) were dissolved in distilled water to make stock solutions of 10-100 mM; aliquots of the stock solutions were then diluted in superfusate to various final concentrations for experimentation. Solutions' pH values were measured after addition of the drugs and readjusted to 7.4.

(LCMP-00276-2006.R2) 9

Statistical analysis. Data are expressed as means \pm standard errors (SE). Statistical analysis was performed using the paired or unpaired Student's *t* test, or ANOVA and post-hoc tests (Student Newman-Keuls, SNK) as indicated. Differences were considered to be significant when $P<0.05$.

Results

Characterization of 40 mM K⁺ (40K)- and PE-induced contraction in isolated rat PA rings.

Raising extracellular K⁺ concentration ([K⁺]_o) from 4.7 to 40 mM (40K), by shifting the K⁺ equilibrium potential (E_K) from -85 to -31 mV and causing membrane depolarization in PASMC, increased active tension in isolated left and right branches of extra-pulmonary arteries (Fig. 1A). Furthermore, extracellular application of the α -adrenergic receptor agonist phenylephrine (PE, 10 μ M) also increased active tension in isolated PA rings (Fig. 1A). The 40K-induced active tension appeared to be slightly greater in the right branch (1253.6±54.8 mg tension/mg wet tissue weight) than in the left branch (1092.7±61.2 mg/mg; n=18, $P=0.06$). However, the PE-mediated active tension, normalized as percentage of the amplitude of 40K-induced tension, was approximately 15.6% smaller in the left branch (66.0±1.9%) than in the right branch (78.2±1.8%; n=18, $P<0.001$) (Fig. 1B).

Removal of extracellular Ca²⁺ almost abolished 40K-induced active tension in PA rings (from 1377.7±55.4 to 43.3±13.9 mg/mg; $P<0.001$), while extracellular application of the voltage-dependent Ca²⁺ channel (VDCC) blocker, nifedipine (Nif, 0.1 μ M) inhibited 40K-induced active tension by approximately 95% (from 1413.9±59.0 to 68.9±25.9 mg/mg; $P<0.001$) (Fig. 2A). Removal of extracellular Ca²⁺ also significantly inhibited PE-induced pulmonary vasoconstriction (Fig. 2B, upper panel). PE-induced active tension in the absence of extracellular Ca²⁺ was 10.3±0.9% of the tension in the presence of extracellular Ca²⁺. That is, removal of extracellular Ca²⁺ decreased PE-mediated PA contraction by 86.7±0.9%, whereas blockade of VDCC with nifedipine only decreased PE-mediated active tension by 55.4±4.5% (Fig. 2B). These results suggest that the 40K-induced pulmonary vasoconstriction is mainly caused by a rise in [Ca²⁺]_{cyt} due to Ca²⁺ influx through the nifedipine-sensitive L-type VDCC, while PE-

induced pulmonary vasoconstriction is caused by a rise in $[Ca^{2+}]_{cyt}$ due to both Ca^{2+} release and Ca^{2+} influx through multiple Ca^{2+} -permeable channels.

PA contraction induced by a rise in $[Ca^{2+}]_{cyt}$ due to capacitative Ca^{2+} entry. In PASMC stimulated by vasoactive agonists (e.g., PE), activation of membrane receptors (e.g., α -adrenergic receptors) stimulates synthesis and production of the second messengers, inositol 1,4,5-trisphosphate (IP_3) and diacylglycerol (DAG) (5, 20). IP_3 induces Ca^{2+} release from the sarcoplasmic reticulum (SR), causing a transient increase in $[Ca^{2+}]_{cyt}$ (7). Depletion of Ca^{2+} from the SR triggers the opening of SOC in the plasma membrane and causes capacitative Ca^{2+} entry (CCE), a unique Ca^{2+} influx mechanism which not only contributes to maintaining the elevated $[Ca^{2+}]_{cyt}$, but also is required for refilling of Ca^{2+} stores (24, 47). In addition to CCE, IP_3 and DAG are also involved in causing Ca^{2+} influx and increasing $[Ca^{2+}]_{cyt}$ by activating second messenger-operated Ca^{2+} channels (SMOC) and/or receptor-operated Ca^{2+} channels (ROC) in the plasma membrane (6, 33, 49). Therefore, the activation of SOC and ROC as well as SMOC all plays a critical role in agonist-mediated increase in $[Ca^{2+}]_{cyt}$ and pulmonary vasoconstriction.

In an isolated PA ring (from the rat main PA) superfused with a Ca^{2+} -free solution, activation of the α -adrenergic receptor by PE caused a transient contraction (Fig. 3A), which was caused by a rise in $[Ca^{2+}]_{cyt}$ due to Ca^{2+} mobilization from the SR. After 5-10 min treatment with the agonist (PE) in the absence of extracellular Ca^{2+} (which would be sufficient to deplete Ca^{2+} from the SR), 1 μM of phentolamine (Phen) was used to block α -adrenergic receptors and to inhibit ROC. Restoration of extracellular Ca^{2+} under these conditions (i.e., the intracellular store is depleted due to PE-mediated Ca^{2+} release, and the receptors and ROC are both inactivated by Phen) caused a contraction due to CCE through SOC. The CCE-mediated contraction (Fig. 3A,

shaded area) accounted for 20-50% of total contraction induced by PE in the presence of extracellular Ca^{2+} . Removal of Phen, or reactivation of the receptor and ROC, caused a further contraction that is due to Ca^{2+} entry through ROC (Fig. 3A). These results indicate that the rise in $[\text{Ca}^{2+}]_{\text{cyt}}$ responsible for agonist-mediated PA contraction results from three major sources: Ca^{2+} release from intracellular store (mainly IP_3 -sensitive SR), Ca^{2+} influx through ROC, and Ca^{2+} influx through SOC (or CCE).

Interestingly, we also found that the CCE-mediated contraction, due to active depletion of intracellular stores with an agonist (e.g., PE), was much greater in the right branches than in the left branches of PA (Fig. 3B). Furthermore, in some PA rings isolated from the right branches, PE (2-20 μM) caused oscillatory contraction that was fully dependent of extracellular Ca^{2+} (Fig. 3C). These results suggest that distribution, expression, and function of, for example, VDCC and SOC/ROC, may differ in PASMC from right and left PA rings.

Studies *in vitro* (28, 39, 70) have demonstrated that intracellular Ca^{2+} stores in PASMC can also be depleted by blockade of the SR $\text{Ca}^{2+}\text{-Mg}^{2+}$ ATPase (SERCA) using cyclopiazonic acid (CPA, 5-10 μM), which subsequently causes CCE or Ca^{2+} influx through SOC. The passive store depletion-mediated CCE elicited a transient contraction in isolated PA rings (right and left branches), whose amplitude was approximately 30% of 40K-induced contraction (Fig. 4A). Although the amplitude of CCE-mediated contraction due to active store depletion (by PE) differed dramatically between right and left branches, the amplitude of CCE-mediated PA contraction due to passive store depletion (by CPA) was comparable (Fig. 4A and B).

Since there is a difference between right and left PA branches in terms of PE- and CCE-induced contraction, we only used the right PA branches for the following experiments.

The thiol oxidant diamide inhibits PA contraction induced by 40K and PE with different IC₅₀. In isolated PA rings (from right branches) preconstricted by 40K (Fig. 5A) or 2 μM PE (Fig. 5B), diamide (1-1,000 μM) caused a dose-dependent inhibition of the active tension. The summarized data shown in Figure 5C indicate that the PE-mediated PA contraction was much more sensitive to diamide than the 40K-mediated contraction. The IC₅₀ of diamide was approximately 335 μM for 40K-mediated contraction, whereas 58 μM for PE-induced PA contraction (Fig. 5C). These results suggest that diamide may affect 40K- and PE-induced PA contraction through different mechanisms.

To determine whether diamide-mediated relaxing effect on isolated PA is due to thiol oxidation, we examined whether DL-dithiothreitol (DTT), a thiol reductant, is able to reverse the diamide-mediated effect. As shown in Figure 6, treatment with 1 mM DTT abolished diamide-mediated PA relaxation. The reversible effect of DTT on diamide-mediated pulmonary vasodilation indicates that diamide causes relaxation in isolated PA rings by inducing thiol oxidation.

Diamide inhibits PE-induced PA contraction by a cGMP/PKG-independent mechanism. In isolated PA rings precontracted by PE, application of the membrane permeable cGMP, 8-Br-cGMP, an activator of protein kinase G (PKG), significantly reduced PE-mediated active tension (from 1019.7±110.5 to 642.8±81.9 mg/mg; P<0.01). However, in the presence of 8-Br-cGMP, diamide still caused a 78% inhibition of PE-mediated pulmonary vasoconstriction. The PE-induced active tension was 642.8±81.9 and 141.8±26.1 mg/mg before and during treatment with 100 μM diamide in the presence of 8-Br-cGMP (Fig. 7A and B). These results indicate that 8-Br-cGMP has little effect on diamide-mediated PA relaxation. Furthermore, pretreatment of the

vessels with HA-1004 (30 μ M) also failed to abolish the diamide-mediated PA relaxation. As shown in Figure 7 (C and D), In PA rings treated with HA-1004, diamide (100 μ M) still caused 76% reduction of PE-induced active tension (from 362.6 \pm 103.7 to 88.4 \pm 52.5 mg/mg; $P<0.001$).

HA-1004 is an inhibitor of serine/threonine protein kinases that inhibits cAMP-dependent kinase (PKA), cGMP-dependent kinase (PKG), and protein kinase C (PKC) with different potency. Ki values for PKA, PKC and PKG are 1.2-2.3, 40, and 0.48-1.3 μ M, respectively, indicating that PKG/PKA are more sensitive to HA-1004 than PKC (22, 38). In our study, we used 30 μ M HA-1004 which would be sufficient to inhibit both PKG and PKA. Therefore, the results shown in Figure 7 suggest that diamide may cause PA relaxation by a cGMP/PKG- or cAMP/PKA-independent pathway.

Diamide-mediated PA relaxation depends on transmembrane K⁺ gradient. As shown in Figure 8, elevation of extracellular [K⁺] ($[K^+]_o$) from 25 mM (25K) to 80 mM (80K) increased the high K⁺-induced active tension, but markedly inhibited diamide-mediated PA relaxation. For example, diamide caused a 34.4 \pm 3.3% reduction of active tension in PA rings preconstricted by 25K, but only caused a 7.2 \pm 1.6% reduction of active tension in PA constricted by 80 K ($P<0.001$; Fig. 8A and B). The dose-response curves of high K⁺-induced PA contraction (Fig. 8C, open circles) and diamide-mediated PA relaxation (Fig. 8C, solid circles) show that the amplitude of K⁺-induced contraction is inversely proportional to the amplitude of diamide-induced PA relaxation when extracellular [K⁺] increases from 20 to 80 mM. These results indicate that diamide-mediated pulmonary vasodilation depends on (or is regulated by) the concentration gradient of K⁺ across the plasma membrane. A decrease of the transmembrane K⁺

gradient (or the K^+ driving force), for example, by raising extracellular $[K^+]$, inhibits diamide-mediated PA contraction.

Increasing PE concentration, which augmented the amplitude of PE-mediated PA contraction, did not significantly affect the amplitude of diamide-mediated PA relaxation (Fig. 9). For example, diamide caused a $56.3\pm3.5\%$ reduction of active tension in PA rings constricted by 0.03 μM PE, while causing a $44.4\pm9.3\%$ reduction of active tension in PA constricted by 100 μM PE ($P=0.35$; Fig. 9A and B). The dose response curve of diamide-induced relaxation is not correlated with the dose response curve of PE-induced PA contraction (Fig. 9C). The diamide-induced PA relaxation was maintained at the same range in PA rings constricted by 0.03-100 μM PE, while the PE-induced active tension increased by approximately 8.5 fold (from 74.2 ± 39.2 mg/mg at 0.03 μM PE to 704.7 ± 54.3 mg/mg at 100 μM PE) (Fig. 9C). These results indicate that the inhibitory effect of high extracellular $[K^+]$ (e.g., by raising extracellular $[K^+]$ from 20 to 80 mM) on diamide-mediated relaxation is unlikely due to enhanced amplitude of active tension, but likely due to reduced K^+ efflux through the plasma membrane.

Similar to the effect of diamide on PA rings preconstricted by 25K and 80K, opening of K^+ channels with cromakalim, an opener of ATP-sensitive K^+ (K_{ATP}) channels in vascular smooth muscle cells, significantly inhibited 25K-mediated PA contraction, but had little effect on 80K-induced PA contraction (Fig. 10). As mentioned above, an increase of extracellular $[K^+]$ reduces the transmembrane K^+ gradient, inhibits K^+ efflux, and attenuates membrane hyperpolarization or repolarization induced by agonists that open K^+ channels. The similar inhibition of diamide- and cromakalim-mediated PA relaxation by increasing extracellular $[K^+]$ from 25 to 80 mM (Fig. 10) further suggests that diamide may cause PA relaxation by opening K^+ channels in the plasma membrane of PASMC.

Diamide increases whole-cell K⁺ currents. To examine whether diamide activates K⁺ channels, we measured whole-cell K⁺ currents in rat pulmonary artery smooth muscle cells (PASMC) before and during treatment with diamide. In PASMC dialyzed and superfused with Ca²⁺-free solutions, extracellular application of 100 μM diamide caused a 29±5% (n=9) increase in the amplitude of transient K⁺ currents and a 25±3% increase in the amplitude of steady-state K⁺ currents (Fig. 11A *a* and *b*). Furthermore, extracellular application of hydrogen peroxide (H₂O₂, 50 μM), a stable reactive oxygen species that causes oxidation of essential thiol groups (19, 46), also significantly increased amplitude of outward K⁺ currents in H9c2 cells (Fig. 11B *a* and *b*). The H₂O₂-sensitive K⁺ currents were also sensitive to 4-aminopyridine (4-AP, 5 mM), a blocker of voltage-gated K⁺ (K_v) channels at concentrations of 1-5 mM (45) (Fig. 11). These results, which are in good agreement with the observations by other investigators (8, 41, 53, 73), suggest that opening of K⁺ channels is involved in pulmonary vasodilation induced by thiol oxidation.

Diamide-mediated PA relaxation is independent of endothelium. Pulmonary vascular tone or excitation-contraction coupling is not only regulated by function of smooth muscle cells but also by vasoactive substances synthesized and released from endothelial cells. Acetylcholine (ACh) is an **muscarinic (M)** receptor agonist that stimulates synthesis and release of nitric oxide (NO) from endothelial cells and causes pulmonary vasodilation. In PA rings with intact endothelium (+*Endo*), extracellular application of ACh (10 μM) caused a 70-80% reduction of 25K-mediated active tension; the ACh-mediated relaxation was almost abolished in endothelium-denuded PA rings (-*Endo*) (Fig. 12A). Functional removal of endothelium in PA rings, **which** abolished ACh-mediated PA relaxation, did not eliminate diamide-mediated relaxation (Fig. 12A).

However, diamide-mediated PA relaxation (inhibition of 25K-mediated PA contraction) was different in PA rings with (+*Endo*) or without (-*Endo*) endothelium. The rate of diamide-induced decrease in active tension was decelerated in endothelium-denuded PA rings (Fig. 12B), while the amplitude of diamide-mediated relaxation was increased in endothelium-denuded rings (-56±3%) in comparison to endothelium-intact rings (-43±3%; $P<0.01$) (Fig. 12C). These results indicate that diamide-mediated PA relaxation is independent of functionally intact endothelium, but modulated by endothelium-derived relaxing and/or constricting factors.

Diamide inhibits CCE-mediated PA contraction. Ca^{2+} influx through SOC or CCE can be induced by active (e.g., via PE-induced IP_3 production) and passive (e.g., via CPA-mediated SEARCA inhibition) depletion of intracellular stores in PASMC (39, 70). Activation of membrane receptors, such as α -adrenergic receptors by PE, increases intracellular IP_3 production, which subsequently activates IP_3 receptors on the SR membrane, induces Ca^{2+} release, and ultimately depletes Ca^{2+} from the SR. Moreover, inhibition of the SR $\text{Ca}^{2+}\text{-Mg}^{2+}$ ATPase (SERCA) by CPA inhibits Ca^{2+} sequestration and leads to passive Ca^{2+} leakage from the SR to the cytosol. Based on our experiments in single PASMC, it usually takes approximately 10-15 min to deplete Ca^{2+} from the SR after treatment with CPA in the absence of extracellular Ca^{2+} . As described earlier, CCE, regardless of its initial cause (either by active or passive depletion of intracellular stores), induces PA contraction.

In PA rings isolated from the right branches, PE caused a transient contraction in the absence of extracellular Ca^{2+} . Approximately 30 min later, restoration of extracellular Ca^{2+} in the presence of the α -adrenergic receptor blocker phentolamine (Phen, 1 μM) caused a sustained PA contraction due to CCE (Fig. 13Aa). The CCE-induced PA contraction, induced by active store

depletion, was significantly inhibited by treatment with 100 μM diamide (Fig. 13Ab). The summarized data show that the PE-mediated transient PA contraction was not significantly changed along time; the active tension in the absence of Ca^{2+} was 372.2 ± 50.1 mg/mg ($n=12$) when the vessels were first challenged with PE (*1st*) and 330.9 ± 47.9 ($n=12$; $P=0.56$) when the vessels were challenged with PE 15 min later (*2nd*) (Fig. 13Ba). The CCE-induced active tension associated with the first PE challenge was 147.9 ± 18.3 mg/mg ($n=12$, without treatment with diamide) and the CCE-induced active tension associated with the second PE challenge was 23.8 ± 6.8 mg/mg ($n=12$; $P<0.001$) in the presence of 100 μM diamide (Fig. 13Bb). These results show that diamide significantly inhibited CCE-mediated PA contraction and the relaxant effect of diamide was not related to changes of PA contractility along time.

To confirm that CCE-dependent contractions were similar between the first and second challenge, we measured and compared the amplitude of CCE-induced PA contraction 60-90 min after the first challenge. As shown in Figure 14, the amplitude of CCE-dependent contraction induced by the second challenge was reduced by $31.9 \pm 5.6\%$ in comparison to the amplitude of CCE-induced contraction induced by the first challenge. However, in PA rings treated with diamide, the amplitude of CCE-induced PA contraction was reduced by $78.9 \pm 7.0\%$ in comparison to the amplitude of CCE-induced PA contraction before diamide treatment (Fig. 13Bb). The difference between challenges in control PA rings ($31.9 \pm 5.6\%$) is significantly smaller than the difference between challenges in PA rings before and after treatment with diamide ($78.9 \pm 7.0\%$; $P<0.001$). These data indicate that the inhibitory effect of diamide on CCE-induced PA contraction is not simply due to a decrease in responsiveness of PA rings over time.

In PA rings isolated from the right branches, treatment with the SERCA inhibitor CPA (50 μ M) in the absence of extracellular Ca^{2+} gradually depleted intracellular stores due to passive Ca^{2+} leakage from the SR to the cytosol. After 20-25 min treatment with CPA, restoration of extracellular Ca^{2+} caused a transient contraction due to CCE (Fig. 15Aa; shadowed area). The increase in active tension induced by CCE (caused by passive store depletion) was also significantly inhibited by diamide (Fig. 15Ab). As shown in Figure 12B, the high K^+ -induced active tension was not significantly changed when the vessels were first challenged with 40K (1st) and challenged 15 min later (2nd) (Fig. 15Ba); however, the CCE-mediated active tension, induced by CPA-mediated passive store depletion, was significantly decreased by 100 μ M diamide (Fig. 15Bb).

The inhibitory effect of diamide on PA contraction induced by active store depletion ($-78.9 \pm 7.0\%$, n=12) (Fig. 13Bb) appeared to be greater than the effect on PA contraction induced by passive store depletion (-59.6 ± 3.5 , n=8; $P < 0.05$) (Fig. 15Bb). These results demonstrate that the thiol oxidant diamide attenuates CCE-induced PA contraction induced by both active and passive store depletion, implying that the relaxant effect of diamide is due to inhibition of store depletion-mediated Ca^{2+} entry, rather than to inhibition of Ca^{2+} mobilization.

Diamide negligibly affects 80K-induced PA constriction. In coronary artery, Iesaki and Wolin (26) reported that diamide-mediated vasodilation is attenuated by L-type Ca^{2+} channel blockers (nifedipine and diltiazem). Therefore, diamide may function through activating a thiol oxidation mechanism that inhibits L-type voltage-dependent Ca^{2+} channels (VDCC) and causes coronary arterial relaxation. To examine whether diamide causes pulmonary vasodilation by inhibiting L-

type Ca^{2+} channels, we examined the effect of high dose of diamide (300 μM) on 80K-induced active tension.

In PA rings preconstricted by 80K, the equilibrium potential for K^+ (E_K) is shifted to -14 mV, which is beyond the threshold (approximately -30 mV) for opening VDCC in PASMC (59). Therefore, the 80K-induced PA constriction is mainly caused by Ca^{2+} influx through L-type VDCC. Under these conditions (i.e., in PA rings constricted by 80K), although opening of K^+ channels shifts the membrane potential (E_m) close to the E_K , it would not be sufficient to close VDCC because the E_K (-14 mV) is less negative than the voltage threshold (-30 mV) for opening VDCC. Furthermore, in PA rings preconstricted by 80K, SOC is not activated because intracellular stores are not depleted and Ca^{2+} entry through voltage-independent cation channels is actually inhibited because of reduced driving force (or transmembrane electrochemical gradient) for Ca^{2+} .

As shown in Figure 16, diamide (300 μM) had no relaxant effect on PA rings preconstricted by 80K, whereas nifedipine (0.1 μM) almost abolished the 80K-induced PA contraction. These data suggest that diamide-mediated thiol oxidation is unlikely involved in inhibiting L-type VDCC in rat pulmonary vascular smooth muscle. The relaxing effect of diamide on PA rings preconstricted by 20-40K (in which the E_K is from -49 to -31 mV) was thus mainly due to opening of K^+ channels (which would shift the E_m close to the E_K and close VDCC) and to other intracellular mechanisms (e.g., inhibition of myosin light chain kinases and contractile proteins). The relaxing effect of diamide on PA rings preconstricted by PE was thus mainly due to inhibition of receptor-operated and/or store-operated Ca^{2+} channels.

Discussion

A rise in $[Ca^{2+}]_{cyt}$ in PASMC is a major trigger for pulmonary vasoconstriction. Upon activation of membrane receptors, agonist-mediated increases in $[Ca^{2+}]_{cyt}$ involve both Ca^{2+} mobilization from intracellular stores (mainly the SR) and Ca^{2+} influx through plasmalemmal Ca^{2+} channels (and transporters). Changes in cellular redox status or in production of oxygen radicals and thiol oxidants have been demonstrated to regulate pulmonary vascular tone (3, 35, 68, 80).

Using isolated PA rings, we showed that membrane depolarization by raising extracellular $[K^+]$ ($[K^+]_o$) (from 4.7 to 20-80 mM) causes sustained vasoconstriction due to Ca^{2+} influx through nifedipine-sensitive L-type VDCC. Furthermore, activation of the α -adrenergic receptor by PE increases $[Ca^{2+}]_{cyt}$ in PASMC and causes pulmonary vasoconstriction by at least three mechanisms: *i*) Ca^{2+} release from the SR, *ii*) store depletion-mediated Ca^{2+} influx through SOC or CCE, and *iii*) Ca^{2+} influx through ROC. The CCE-mediated pulmonary vasoconstriction can also be induced by passive depletion of intracellular Ca^{2+} stores using the SERCA inhibitor, CPA. Finally, the CCE-mediated active tension appears to be predominant in the right branches of PA, while high K^+ -induced active tension is comparable between right and left PA branches. In other words, CCE-induced PA contraction due to passive versus active store depletion differs between left and right branches. While the passive store depletion-mediated PA contraction (by CPA) is comparable, the active store depletion-induced contraction is significantly greater in right PA branches than in left branches.

Furthermore, our results demonstrated that: *a*) acute treatment with the thiol oxidant, diamide, causes pulmonary vasodilation; *b*) the relaxing effect of diamide is not dependent of intact endothelium but modulated by endothelium-derived factors; *c*) pretreatment of the vessels

with the membrane permeable PKG/PKA inhibitor, HA-1004, negligibly affects diamide-mediated pulmonary vasodilation; *d*) the thiol oxidant-mediated pulmonary vasodilation is markedly inhibited when extracellular $[K^+]$ is raised (e.g., from 20 to 80 mM) **and thus** the transmembrane K^+ driving force is reduced; and *e*) the diamide-induced pulmonary vasodilation is abolished in vessels constricted with 80 mM K^+ . These results indicate that thiol oxidation by diamide induces pulmonary vasodilation by opening K^+ channels (and subsequent membrane hyperpolarization) and blocking SOC that are opened by active and passive store depletion. While diamide indirectly inhibits VDCC activity by causing membrane hyperpolarization or repolarization (53, 73), thiol oxidation appears not to have **a** direct inhibitory effect on VDCC because diamide negligibly affected active tension in PA rings **contracted** by 80 mM K^+ .

Diamide is an oxidant that crosses the plasma membrane rapidly by diffusion and promotes thiol oxidation of membrane and intracellular proteins (31). Diamide decreases **the** GSH/GSSG ratio by oxidizing intracellular GSH to glutathione disulfide (GSSG) (30), and decreases **the** NADPH/NADP⁺ ratio by inhibiting NADPH generation (42). The thiol oxidant diamide has been demonstrated to stimulate soluble guanylate cyclase (sGC) in platelets at low concentrations and to inhibit the sGC activity at higher concentrations (74). In bovine pulmonary arteries, Mingone et al. provide compelling evidence that the thiol oxidant diamide (1 mM) inhibits the ability of nitric oxide (NO) to activate sGC, and attenuates NO-mediated pulmonary vasodilatation (42). Our results, however, indicate that treatment of rat PA rings with 8-Br-cGMP or with HA-1004, a PKG/PKA inhibitor, failed to abolish diamide (100 μ M)-mediated PA relaxation. These results suggest that, in addition to inhibiting sGC activation, the thiol oxidant may have **a** direct oxidizing effect on membrane ion channels (53). Indeed, our results imply that thiol oxidation by diamide causes pulmonary vasodilation by opening K^+ channels and by

inhibiting SOC in the plasma membrane of PASMC. It remains unclear how the thiol oxidant-mediated cellular redox changes in PASMC cause opposite effect on K⁺ channels and store depletion-activated Ca²⁺ channels.

PASMC functionally express multiple K⁺ channels, including voltage-gated K⁺ (K_V) channels, Ca²⁺-activated K⁺ (K_{Ca}) channels, ATP-sensitive K⁺ channels, and inward rectifier K⁺ (K_{IR}) channels (63). In PA rings constricted by, for example, 20K, opening of any K⁺ channels would shift membrane potential towards the K⁺ equilibrium potential (E_K), which is estimated to be approximately -49 mV (given that intracellular [K⁺] is 140 mM), close VDCC (the activation threshold for VDCC is approximately -40 to -30 mV; the peak of window currents is approximately -25 to -15 mV) (17, 45, 58), and cause PASMC relaxation. In PA rings constricted by 80 mM K⁺, however, opening of K⁺ channels would only shift the membrane potential towards -14 mV (the calculated E_K in PASMC superfused with 80 mM K⁺-containing solution) and **would** therefore **be** unable to close VDCC and cause PASMC relaxation. As shown in Figures 8 and 16, increase of extracellular [K⁺] from 20 to 80 mM increased the active tension in PA rings, but significantly decreased diamide-mediated PA relaxation. These data strongly indicate that diamide causes pulmonary vasodilation by opening K⁺ channels in PASMC. The oxidation-mediated opening of different types of K⁺ channels (e.g., K_V, K_{ATP}, and K_{Ca} channels) is well known (4, 48, 65), and oxidation of thiol or sulfide hydrogen (-SH) groups to form disulfide bridges may cause conformational changes in the channel protein and open the channel by modulation its gating or inactivation kinetics (53, 57, 80).

In bovine coronary arteries, Iesaki and Wolin (26) reported that diamide-mediated vasodilation was significantly inhibited in arteries constricted by high K⁺ in comparison to arteries constricted by agonist (e.g., U46619). These observations further support our contention

that diamide at least in part causes vasodilation by opening K⁺ channels in PASMC, which subsequently induces membrane hyperpolarization (or repolarization), closure of voltage-dependent L-type Ca²⁺ channels, and inhibition of Ca²⁺ influx. Furthermore, Iesaki and Wolin demonstrated that blockade of voltage-dependent L-type Ca²⁺ channels with nifedipine (1 μM) or diltiazem (10 μM) inhibited diamide-mediated vasodilation in bovine coronary arteries preconstricted by U46619 (26), suggesting that thiol oxidation-mediated vasodilation may be partially induced by inhibiting L-type Ca²⁺ channels. In rat PA rings, however, diamide (100 or 300 μM) had a negligible effect on 80K-mediated vasoconstriction (Figs. 8 and 16), which is mainly caused by Ca²⁺ influx through voltage-dependent L-type Ca²⁺ channels in PASMC. It is possible that thiol oxidation induced by diamide may target different Ca²⁺ channels in different arteries (e.g., pulmonary vs. coronary arteries) or in pulmonary arteries isolated from different species. Another possibility that nifedipine or diltiazem attenuates diamide-induced coronary arterial relaxation (26) is because of the potential non-selective inhibitory effect of high doses of nifedipine and diltiazem on store-operated and receptor-operated Ca²⁺ channels.

Studies on the molecular identification of store-operated Ca²⁺ channels indicate that multiple channel subunits participate in forming functional SOC in vascular smooth muscle and endothelial cells (14, 15, 29, 36, 60, 69, 76). Transient receptor potential (*TRP*) genes have been demonstrated to encode the channel subunits that are involved in the formation of functional SOC in human and animal PASMC (10, 77, 78). Similar to the pore-forming Kv channel α subunit, the TRP channel subunit also contains a cytoplasmic N-terminus, six transmembrane domains (S1 to S6), a pore region between S5 and S6 domains, and a cytoplasmic C-terminus. The functional TRP channels or *TRP*-encoded SOC are either homotetramers or heterotetramers; thus differences in composition may determine the channel's sensitivity to store depletion or

receptor activation. As shown in Figures 13 and 15, the thiol oxidant diamide not only inhibited CCE-induced PA contraction due to PE-mediated active store depletion (Fig. 13), but also attenuated CCE-induced PA contraction due to CPA-mediated passive store depletion (Fig. 15). The greater inhibition on PA contraction induced by active store depletion than that induced by passive store depletion implies that diamide-mediated PA relaxation may involve inhibition of agonist-mediated receptor activation and downstream signaling cascades.

In porcine aortic endothelial cells, Posteser et al. (52) demonstrated that TRPC3 and TRPC4 formed a redox-sensitive heterotetrameric cation channel, indicating that TRPC3 and TRPC4 are involved in forming native cation channels that are regulated by the cellular redox state. The TRPC3/TRPC4 channels over-expressed in porcine aortic endothelial cells and HEK-293 cells could be activated by incubation with carbachol (200 µM), cholesterol oxidase (0.5 U/ml), or 1-oleoyl-2-acetyl-*sn*-glycerol (100 µM, an analogue of diacylglycerol). Our data in isolated PA rings suggest that thiol oxidation induced by diamide may cause pulmonary vasodilation by closing SOC in PASMC. Further study is thus needed to define *a*) whether the TRPC3/TRPC4 heterotetrameric channels in PASMC are regulated by the cellular redox state in the same way as they are in vascular endothelial cells, *b*) whether TRPC3 and TRPC4 homo- and hetero-tetrameric channels in PASMC are regulated indirectly by a redox-sensitive intermediate, and *c*) whether canonical TRP channels functionally expressed in PASMC can be oppositely regulated by different reducing agents.

Acute hypoxia causes pulmonary vasoconstriction, which is believed to be a unique and intrinsic property of PASMC. It has been demonstrated that hypoxia-induced pulmonary vasoconstriction is associated with inhibition of Kv channels (2, 51, 80) and activation of TRP or SOC channels (13, 70). Hypoxia-mediated changes in cellular redox status (determined by the

ratios of NAD(P)H/NAD(P) and GSH/GSSG) are likely an important mechanism by which acute hypoxia inhibits Kv channels and activates TRP channels in PASMC (16, 34, 70). It is still controversial whether hypoxia leads to a decreased or an increased production of reactive oxygen species (ROS) and how changes in ROS production affect cellular response. However, studies *in vitro* demonstrate that whole-cell K⁺ currents in rat PASMC were increased by intracellular application of oxidized glutathione (GSSG), but decreased by reduced glutathione (GSH) (73, 80). In addition, NADH decreases the single-channel activity of K_{Ca} channels in PASMC, whereas NAD increases the channel activity (34). The mechanism by which hypoxia or redox status change modulates Kv channel activity appears to involve the cytoplasmic β-subunit, which contains an active oxidoreductase domain with a NADPH cofactor pocket and a substrate binding site (18). Therefore, the Kv channel β subunit may be an important target for the thiol oxidant diamide, ROS and/or redox status changes to affect Kv channel function (4).

In summary, the data from this study present evidence that thiol oxidation of membrane proteins and intracellular enzymes in PASMC play an important role in regulating pulmonary vascular tone. The thiol oxidant diamide causes pulmonary vasodilation by potentially opening K⁺ channels and inhibiting SOC in PASMC; the thiol oxidation-mediated effect appears to be independent of cellular cGMP/PKG and intact endothelium. Our observations also indicate that shifting the redox status in PASMC to a more oxidized level leads to pulmonary arterial relaxation.

Acknowledgments:

This work was supported in part by the grants from the National Heart, Lung, and Blood Institute of the National Institutes of Health (HL066012, HL054043 and HL064945). We thank A. Nicholson for technical assistance.

References

1. **Aaronson PI, Robertson TP, and Ward JPT.** Endothelium-derived mediators and hypoxic pulmonary vasoconstriction. *Respir Physiol Neurobiol* 132: 107-120, 2002.
2. **Archer SL, Huang J, Henry T, Peterson D, and Weir EK.** A redox-based O₂ sensor in rat pulmonary vasculature. *Circ Res* 73: 1100-1112, 1993.
3. **Archer SL, Will JA, and Weir EK.** Redox status in the control of pulmonary vascular tone. *Herz* 11: 127-141, 1986.
4. **Bähring R, Milligan CJ, Vardanyan V, Engeland B, Young BA, Dannenberg J, Waldschütz R, Edwards JP, Wray D, and Pongs O.** Coupling of voltage-dependent potassium channel inactivation and oxidoreductase active site of Kv_b subunits. *J Biol Chem* 276: 22923-22929, 2001.
5. **Berridge MJ.** Inositol trisphosphate and calcium signaling. *Nature* 361: 315-325, 1993.
6. **Birnbaumer L, Zhu X, Jiang M, Boulay G, Peyton M, Vannier B, Brown D, Platano D, Sadeghi H, Stefani E, and Birnbaumer M.** On the molecular basis and regulation of cellular capacitative calcium entry: Roles for Trp proteins. *Proc Natl Acad Sci USA* 93: 15195-15202, 1996.
7. **Boulay G, Brown DM, Qin N, Jiang M, Dietrich A, Zhu MX, Chen Z, Birnbaumer M, Mikoshiba K, and Birnbaumer L.** Modulation of Ca²⁺ entry by polypeptides of the inositol 1,4,5-trisphosphate receptor (IP₃R) that bind transient receptor potential (TRP): Evidence for roles of TRP and IP₃R in store depletion-activated Ca²⁺ entry. *Proc Natl Acad Sci USA* 96: 14955-14960, 1999.
8. **Burke-Wolin T and Wolin MS.** H₂O₂ and cGMP may function as an O₂ sensor in the pulmonary artery. *J Appl Physiol* 66: 167-170, 1989.
9. **Chen G, Suzuki H, and Weston AH.** Acetylcholine releases endothelium-derived hyperpolarizing factor and EDRF from rat blood vessels. *Br J Pharmacol* 95: 1165-1174, 1988.
10. **Cioffi DL, Wu S, Alexeyev M, Goodman SR, Zhu MX, and Stevens T.** Activation of the endothelial store-operated *I_{SOC}* Ca²⁺ channel requires interaction of protein 4.1 with TRPC4. *Circ Res* 97: 1164-1172, 2005.
11. **Cornfield DN, Stevens T, McMurry IF, Abman SH, and Rodman DM.** Acute hypoxia increases cytosolic calcium in fetal pulmonary artery smooth muscle cells. *Am J Physiol* 265: L53-L56, 1993.
12. **Ekhterae D, Platoshyn O, Zhang S, Remillard CV, and Yuan JX-J.** Apoptosis repressor with caspase domain inhibits cardiomyocyte apoptosis by reducing voltage-gated K⁺ currents. *Am J Physiol Cell Physiol* 284: C1405-C1410, 2003.
13. **Fantozzi I, Zhang S, Platoshyn O, Remillard CV, Cowling RT, and Yuan JX-J.** Hypoxia increases AP-1 binding activity by enhancing capacitative Ca²⁺ entry in human pulmonary artery endothelial cells. *Am J Physiol Lung Cell Mol Physiol* 285: L1233-L1245, 2003.
14. **Fasolato C and Nilius B.** Store depletion triggers the calcium release-activated calcium current (I_{CRAC}) in macrovascular endothelial cells: a comparison with Jurkat and embryonic kidney cell lines. *Pflügers Arch - Eur J Physiol* 436: 69-74, 1998.
15. **Feske S, Gwack Y, Prakriya M, Srikanth S, Poppel S-H, Tanasa B, Hogan PG, Lewis RS, Daly M, and Rao A.** A mutation in Orai1 causes immune deficiency by abrogating CRAC channel function. *Nature* 441: 179-185, 2006.

16. **Filomeni G, Rotilio G, and Ciriolo MR.** Cell signalling and the glutathione redox system. *Biochem Pharmacol* 64: 1057-1064, 2002.
17. **Fleischmann BK, Murray RK, and Kotlikoff MI.** Voltage window for sustained elevation of cytosolic calcium in smooth muscle cells. *Proc Natl Acad Sci USA* 91: 11914-11918, 1994.
18. **Gulbis JM, Mann S, and MacKinnon R.** Structure of a voltage-dependent K⁺ channel b subunit. *Cell* 97: 943-952, 1999.
19. **Gupte SA and Wolin MS.** Interaction of oxidants with pulmonary vascular signaling systems. In: *Hypoxic Pulmonary Vasoconstriction: Cellular and Molecular Mechanisms*, edited by Yuan JX-J. Boston, MA: Kluwer Academic Publishers, 2002, p. 242-262.
20. **Hamada H, Damron DS, Hong SJ, Van Wagoner DR, and Murray PA.** Phenylephrine-induced Ca²⁺ oscillations in canine pulmonary artery smooth muscle cells. *Circ Res* 81: 812-823, 1997.
21. **Han C, Abel PW, and Minneman KP.** α_1 -Adrenoceptor subtypes linked to different mechanisms for increasing intracellular Ca²⁺ in smooth muscle. *Nature* 329: 333-335, 1987.
22. **Hidaka H, Inagaki M, Kawamoto S, and Sasaki Y.** Isoquinolinesulfonamides, novel and potent inhibitors of cyclic nucleotide dependent protein kinase and protein kinase C. *Biochemistry* 23: 5036-5041, 1984.
23. **Himpens B, Matthijs G, and Somlyo AP.** Desensitization to cytoplasmic Ca²⁺ and Ca²⁺ sensitivities of guinea-pig ileum and rabbit pulmonary artery smooth muscle. *J Physiol* 413: 489-503, 1989.
24. **Hoth M and Penner R.** Depletion of intracellular calcium stores activates a calcium current in mast cells. *Nature* 355: 353-356, 1992.
25. **Hughes AD.** Calcium channels in vascular smooth muscle cells. *J Vasc Res* 32: 353-370, 1995.
26. **Iesaki T and Wolin MS.** Thiol oxidation activates a novel redox-regulated coronary vasodilator mechanism involving inhibition of Ca²⁺ influx. *Arterioscler Thromb Vasc Biol* 20: 2359-2365, 2000.
27. **Ignarro LJ, Buga GM, Wood KS, Byrns RE, and Chaudhuri G.** Endothelium-derived relaxing factor produced and released from artery and vein is nitric oxide. *Proc Natl Acad Sci USA* 84: 9265-9269, 1987.
28. **Janiak R, Wilson SM, Montague S, and Hume JR.** Heterogeneity of calcium stores and elementary release events in canine pulmonary arterial smooth muscle cells. *Am J Physiol Cell Physiol* 280: C22-C33, 2001.
29. **Kimura C, Cheng W, Hisadome K, Wang Y-P, Koyama T, Karashima Y, Oike M, and Ito Y.** Superoxide anion impairs contractility in cultured aortic smooth muscle cells. *Am J Physiol Heart Circ Physiol* 283: H382-Ha390, 2002.
30. **Kosower NS and Kosower EM.** Diamide: an oxidant probe for thiols. *Methods Enzymol* 251: 123-133, 1995.
31. **Kosower NS, Kosower EM, Wertheim B, and Correa WS.** Diamide, a new reagent for the intracellular oxidation of glutathione to the disulfide. *Biochem Biophys Res Comm* 37: 593-596, 1969.
32. **Kovitz KL, Aleskowitch TD, Sylvester JT, and Flavahan NA.** Endothelium-derived contracting and relaxing factors contribute to hypoxic responses of pulmonary arteries. *Am J Physiol* 265: H1139-H1148, 1993.

33. **Kuno M and Gardner P.** Ion channels activated by inositol 1,4,5-trisphosphate in plasma membrane of human T-lymphocytes. *Nature* 326: 301-304, 1987.
34. **Lee S, Park M, So I, and Earm YE.** NADH and NAD modulates Ca^{2+} -activated K^+ channels in small pulmonary arterial smooth muscle cells of the rabbit. *Pflügers Arch - Eur J Physiol* 427: 378-380, 1994.
35. **Liska J, Holm P, Owall A, and Franco-Cereceda A.** Endothelin infusion reduces hypoxic pulmonary hypertension in pigs in vivo. *Acta Physiol Scand* 154: 489-498, 1995.
36. **Ma R, Pluznick J, Kudlacek P, and Sansom SC.** Protein kinase C activates store-operated Ca^{2+} channels in human glomerular mesangial cells. *J Biol Chem* 276: 25759-25765, 2001.
37. **Madden JA, Vadula KS, and Kurup VP.** Effects of hypoxia and other vasoactive agents on pulmonary and cerebral artery smooth muscle cells. *Am J Physiol* 263: L384-L393, 1992.
38. **Matuszyk J, Cebrat M, Kalas W, and Strzadala L.** HA1004, an inhibitor of serine/threonine protein kinases, restores the sensitivity of thymic lymphomas to Ca^{2+} -mediated apoptosis through a protein kinase A-independent mechanism. *Int Immunopharmacol* 2: 435-442, 2002.
39. **McDaniel SS, Platoshyn O, Wang J, Yu Y, Sweeney M, Krick S, Rubin LJ, and Yuan JX-J.** Capacitative Ca^{2+} entry in agonist-induced pulmonary vasoconstriction. *Am J Physiol Lung Cell Mol Physiol* 280: L870-L880, 2001.
40. **McMurtry IF, Davidson AB, Reeves JT, and Grover RF.** Inhibition of hypoxic pulmonary vasoconstriction by calcium antagonists in isolated rat lungs. *Circ Res* 38: 99-104, 1976.
41. **Michelakis ED, Hampl V, Nsair A, Wu XC, Harry G, Haromy A, Gurtu R, and Archer SL.** Diversity in mitochondrial function explains differences in vascular oxygen sensing. *Circ Res* 90: 1307-1315, 2002.
42. **Mingone CJ, Gupte SA, Ali N, Oeckler RA, and Wolin MS.** Thiol oxidation inhibits nitric oxide-mediated pulmonary artery relaxation and guanylate cyclase stimulation. *Am J Physiol Lung Cell Mol Physiol* 290: L549-L557, 2006.
43. **Moncada S, Gryglewski R, Bunting S, and Vane JR.** An enzyme isolated from arteries transforms prostaglandin endoperoxides to an unstable substance that inhibits platelet aggregation. *Nature* 263: 663-665, 1976.
44. **Murray TR, Chen L, Marshall BE, and Macarak EJ.** Hypoxic contraction of cultured pulmonary vascular smooth muscle cells. *Am J Respir Cell Mol Biol* 3: 457-465, 1990.
45. **Nelson MT, Patlak JB, Worley JF, and Standen NB.** Calcium channels, potassium channels, and voltage dependence of arterial smooth muscle tone. *Am J Physiol* 259: C3-C18, 1990.
46. **Palmer L.** Chemistry of oxygen and its derivatives in the lung. In: *Hypoxic Pulmonary Vasoconstriction: Cellular and Molecular Mechanisms*, edited by Yuan JX-J. Boston, MA: Kluwer Academic Publishers, 2004, p. 233-245.
47. **Parekh AB and Penner R.** Store depletion and calcium influx. *Physiol Rev* 77: 901-930, 1997.
48. **Park MK, Lee SH, Lee SJ, Ho W-K, and Earm YE.** Different modulation of Ca^{2+} -activated K^+ channels by the intracellular redox potential in pulmonary and ear arterial smooth muscle cells of the rabbit. *Pflügers Arch - Eur J Physiol* 430: 308-314, 1995.

49. **Penner R, Matthews G, and Neher E.** Regulation of calcium influx by second messengers in rat mast cells. *Nature* 334: 499-504, 1988.
50. **Pietra GG, Edwards WD, Kay JM, Rich S, Kernis J, Schloo B, Ayres SM, Bergofsky EH, Brundage BH, and Detre KM.** Histopathology of primary pulmonary hypertension. A qualitative and quantitative study of pulmonary blood vessels from 58 patients in the National Heart, Lung, and Blood Institute, Primary Pulmonary Hypertension Registry. *Circulation* 80: 1198-1206, 1989.
51. **Post JM, Hume JR, Archer SL, and Weir EK.** Direct role for potassium channel inhibition in hypoxic pulmonary vasoconstriction. *Am J Physiol* 262: C882-C890, 1992.
52. **Poteser M, Graziani A, Rosker C, Eder P, Derler I, Kahr H, Zhu MX, Romanin C, and Groschner K.** TRPC3 and TRPC4 associate to form a redox-sensitive cation channel: evidence for expression of native TRPC3-TRPC4 heteromeric channels in endothelial cells. *J Biol Chem* 281: 13588-13595, 2006.
53. **Reeve HL, Weir EK, Nelson DP, Peterson DA, and Archer SL.** Opposing effects of oxidants and antioxidants on K^+ channel activity and tone in rat vascular tissue. *Exp Physiol* 80: 825-834, 1995.
54. **Remillard CV, Zhang W-M, Shimoda LA, and Sham JSK.** Physiological properties and functions of Ca^{2+} sparks in rat intrapulmonary arterial smooth muscle cells. *Am J Physiol Lung Cell Mol Physiol* 283: L433-L444, 2002.
55. **Rich S, Kaufmann E, and Levy PS.** The effect of high doses of calcium-channel blockers on survival in primary pulmonary hypertension. *N Engl J Med* 327: 76-81, 1992.
56. **Runo JR and Loyd JE.** Primary pulmonary hypertension. *Lancet* 361: 1533-1544, 2003.
57. **Ruppertsberg JP, Stocker M, Pongs O, Heinemann SH, Frank R, and Koenen M.** Regulation of fast inactivation of cloned mammalian $I_K(A)$ channels by cysteine oxidation. *Nature* 352: 711-714, 1991.
58. **Smirnov SV and Aaronson PI.** Ca^{2+} currents in single myocytes from human mesenteric arteries: evidence for a physiological role of L-type channels. *J Physiol* 457: 455-475, 1992.
59. **Smirnov SV, Beck R, Tammaro P, Ishii T, and Aaronson PI.** Electrophysiologically distinct smooth muscle cell subtypes in rat conduit and resistance pulmonary arteries. *J Physiol* 538: 867-878, 2002.
60. **Soboloff J, Spassova MA, Tang XD, Hewavitharana T, Xu W, and Gill DL.** Orai1 and STIM reconstitute store-operated calcium channel function. *J Biol Chem* 281: 20661-20665, 2006.
61. **Somlyo AP and Somlyo AV.** Signal transduction and regulation in smooth muscle. *Nature* 372:231-236, 1994.
62. **Somlyo AV and Somlyo AP.** Electromechanical and pharmacomechanical coupling in vascular smooth muscle. *J Pharmacol Exp Ther* 159: 129-145, 1968.
63. **Standen NB and Quayle JM.** K^+ channel modulation in arterial smooth muscle. *Acta Physiol Scand* 164: 549-557, 1998.
64. **Thorne GD, Ishida Y, and Paul RJ.** Hypoxic vasorelaxation: Ca^{2+} -dependent and Ca^{2+} -independent mechanisms. *Cell Calcium* 36: 201-208, 2004.
65. **Tokube K, Kiyosue T, and Arita M.** Openings of cardiac K_{ATP} channel by oxygen free radicals produced by xanthine oxidase reaction. *Am J Physiol* 271: H478-H489, 1996.

66. **Tolins M, Weir EK, Chesler E, Nelson DP, and From AH.** Pulmonary vascular tone is increased by a voltage-dependent calcium channel potentiator. *J Appl Physiol* 60: 942-948, 1986.
67. **Vadula MS, Kleinman JG, and Madden JA.** Effect of hypoxia and norepinephrine on cytoplasmic free Ca^{2+} in pulmonary and cerebral arterial myocytes. *Am J Physiol* 265: L591-L597, 1993.
68. **Vejlstrup NG and Dorrington KL.** Intense slow hypoxic pulmonary vasoconstriction in gas-filled and liquid-filled lungs: an in vivo study in the rabbit. *Acta Physiol Scand* 148: 305-313, 1993.
69. **Vig M, Beck A, Billingsley JM, Lis A, Parvez S, Peinelt C, Koomoa DL, Soboloff J, Gill DL, Fleig A, Kinet JP, and Penner R.** CRACM1 multimers form the ion-selective pore of the CRAC channel. *Curr Biol* 16:2073-2079, 2006.
70. **Wang J, Shimoda LA, Weigand L, Wang W, Sun D, and Sylvester JT.** Acute hypoxia increases intracellular $[\text{Ca}^{2+}]$ in pulmonary arterial smooth muscle by enhancing capacitative Ca^{2+} entry. *Am J Physiol Lung Cell Mol Physiol* 288: L1059-L1069, 2005.
71. **Waypa GB and Schumacker PT.** Hypoxic pulmonary vasoconstriction: Redox events in oxygen sensing. *J Appl Physiol* 98: 404-414, 2005.
72. **Weigand L, Foxson J, Wang J, Shimoda LA, and Sylvester JT.** Inhibition of hypoxic pulmonary vasoconstriction by antagonists of store-operated Ca^{2+} and nonselective cation channels. *Am J Physiol Lung Cell Mol Physiol* 289: L5-L13, 2005.
73. **Weir EK, Hong Z, Porter VA, and Reeve HL.** Redox signaling in oxygen sensing by vessels. *Respir Physiol Neurobiol* 132: 121-130, 2002.
74. **Wu XB, Brune B, von Appen F, and Ullrich V.** Reversible activation of soluble guanylate cyclase by oxidizing agents. *Arch Biochem Biophys* 294: 75-82, 1992.
75. **Yanagisawa M, Kurihara H, Kimura S, Tomobe Y, Kobayashi M, Mitsui Y, Yazaki Y, Goto K, and Masaki T.** A novel potent vasoconstrictor peptide produced by vascular endothelial cells. *Nature* 332: 411-415, 1988.
76. **Yeromin AV, Zhang SL, Jiang W, Yu Y, Safrina O, and Cahalan MD.** Molecular identification of the CRAC channel by altered ion selectivity in a mutant of Orai. *Nature* 443: 226-229, 2006.
77. **Yu Y, Fantozzi I, Remillard CV, Landsberg JW, Kunichika N, Platosyn O, Tigno DD, Thistlethwaite PA, Rubin LJ, and Yuan JX-J.** Enhanced expression of transient receptor potential channels in idiopathic pulmonary arterial hypertension. *Proc Natl Acad Sci USA* 101: 13861-13866, 2004.
78. **Yu Y, Sweeney M, Zhang S, Platosyn O, Landsberg J, Rothman A, and Yuan JX-J.** PDGF stimulates pulmonary vascular smooth muscle cell proliferation by upregulating TRPC6 expression. *Am J Physiol Cell Physiol* 284: C316-C330, 2003.
79. **Yuan JX-J and Rubin LJ.** Pathogenesis of pulmonary arterial hypertension: The need for multiple hits. *Circulation* 111: 534-538, 2005.
80. **Yuan X-J, Tod ML, Rubin LJ, and Blaustein MP.** Deoxyglucose and reduced glutathione mimic effects of hypoxia on K^+ and Ca^{2+} conductances in pulmonary artery cells. *Am J Physiol* 267: L52-L63, 1994.
81. **Yuan X-J, Tod ML, Rubin LJ, and Blaustein MP.** Contrasting effects of hypoxia on tension in rat pulmonary and mesenteric arteries. *Am J Physiol* 259: H281-H289, 1990.

(LCMP-00276-2006.R2) 33

82. **Zhang F, Carson RC, Zhang H, Gibson G, and Thomas HMr.** Pulmonary artery smooth muscle cell $[Ca^{2+}]_i$ and contraction: responses to diphenyleneiodonium and hypoxia. *Am J Physiol* 273: L603-L611, 1997.

Figure Legends

Figure 1. Comparison of amplitude of high K⁺- and PE-mediated vasoconstriction in left and right PA branches with intact endothelium. *A:* Representative tracings showing active tension induced by 40 mM K⁺ (40K) or 2 μM PE in left (upper panel) and right (lower panel) PA branches. *B:* Summarized data showing amplitude of the 40K-induced active tension (left panel) and PE-induced active tension normalized to 40K-mediated tension (right panel). *** $P<0.001$ vs. left (n=18 rings).

Figure 2. Excitation-contraction coupling in pulmonary arteries depends on Ca²⁺ influx. *A:* Representative tracings (left panels) and summarized data (means±SD, right panels) showing active tension induced by 40 mM K⁺ (40K) before (Cont), during, and after (Wash) removal of extracellular Ca²⁺ (0Ca, upper panel; n=6) or addition of 0.1 μM nifedipine (Nif, n=12). *** $P<0.001$ vs. control and washout. *B:* Representative tracings (left panels) and summarized data (means±SE, right panels) showing active tension induced by 2 μM phenylephrine (PE) before (Cont), during, and after (Wash) removal of extracellular Ca²⁺ (0Ca, upper panel; n=6) or addition of 0.1 μM nifedipine (Nif, n=10). *** $P<0.001$ vs. control and washout. All PA rings were obtained from right PA branches with intact endothelium.

Figure 3. Pulmonary vasoconstriction induced by capacitative Ca²⁺ entry (CCE) due to active depletion of intracellular stores in different branches of pulmonary artery. *A* and *B:* Representative tracings showing active tension induced by 2 μM PE in the presence and absence (0Ca) of extracellular Ca²⁺ in the main PA (*A*) and the left and right PA branches (*Ba*). Phentolamine (Phen, 1 μM), an α-adrenergic receptor blocker, was applied to the vessels after

PE-mediated transient PA contraction and before restoration of extracellular Ca^{2+} . Shadowed area indicates the increase in active tension due to a rise in $[\text{Ca}^{2+}]_{\text{cyt}}$ via CCE. Summarized data (*Bb*, means \pm SE) showing the amplitude of PE-induced active tension due to Ca^{2+} release (in the absence of extracellular Ca^{2+}) and to CCE (when extracellular Ca^{2+} was restored in the presence of phentolamine) in left (grey bars) and right (solid bars) PA branches (*n=12*). * $P<0.05$ vs. right branches. *C*: A representative tracing showing PE-induced oscillatory contraction in a PA ring isolated from right PA branches.

Figure 4. Comparison of CCE-mediated pulmonary vasoconstriction induced by active and passive store depletion in left and right PA branches. *A*: Representative tracings showing tension changes induced by 40 mM K^+ (40K), CPA (50 μM , in the presence and absence of extracellular Ca^{2+}), and PE (2 μM , in the presence and absence of extracellular Ca^{2+}) in left (upper panel) and right (lower panel) PA branches. Phentolamine (Phen, 1 μM) was applied to the vessels after PE-mediated transient PA contraction and before restoration of extracellular Ca^{2+} . Shadowed area indicates the increase in active tension due to a rise in $[\text{Ca}^{2+}]_{\text{cyt}}$ via CCE mediated by CPA-induced passive store depletion and by PE-induced active store depletion. *B*: Summarized data (means \pm SE) showing the amplitude of CPA- and PE-induced active tension mediated by CCE (left panel; *n=12-17*) and the amplitude of PE-induced active tension after treatment with phentolamine (right panel; *n=12*) in left and right PA branches. ** $P<0.01$, *** $P<0.001$ vs. left branches.

Figure 5. Dose-dependent relaxing effect of diamide on pulmonary vasoconstriction induced by 40 mM K^+ (40K) and phenylephrine (PE, 2 μM). *A* and *B*: Representative tracings showing

tension changes in response to 1-1,000 μM diamide in PA rings constricted by 40K (*A*) and PE (*B*). Diamide was applied to the vessels when 40K- and PE-mediated active tension reached plateau. *C*: Dose-response curves (means \pm SE) showing 40K- and PE-induced active tension (normalized to the maximal tension; $n=4$) in PA rings (right branches) treated before and during treatment with 1, 3, 10, 30, 100, 300, and 1,000 μM diamide. * $P<0.05$ and ** $P<0.01$ vs. PE.

Figure 6. Thiol reductant reverses diamide-induced pulmonary vasodilation. *A*: A representative tracing showing tension changes in a PA ring preconstricted by PE (2 μM) before, during, and after application of diamide (100 μM) alone or diamide and dithiothreitol (DTT, 1 mM). *B*: Summarized data (means \pm SE) showing the amplitude of PE-induced active tension before (Control, open bar) and during application of diamide (solid bar) or diamide+DTT (grey bar; $n=8$). ** $P<0.01$ vs. Control and Diamide+DTT.

Figure 7. Diamide-mediated pulmonary vasodilation is not dependent of cGMP and protein kinase G (PKG). *A*: A representative tracing showing tension changes when diamide (100 μM) was applied after superfusion with 8-Br-cGMP (50 μM) in a PA ring constricted by 2 μM phenylephrine (PE). *B*: Summarized data (means \pm SE; $n=6$) showing the amplitude of PE-induced active tension before (Control), during, and after (Washout) application of 8-Br-cGMP or 8-Br-cGMP and diamide (100 μM). *C*: A representative tracing showing PE (2 μM)-mediated tension change before, during and after application of 100 μM diamide in a PA ring treated with 30 μM HA-1004, an inhibitor of PKG/PKA. *D*: Summarized data (means \pm SE; $n=5$) showing the amplitude of PE-induced active tension before (Control), during, and after (Washout) application of diamide in the presence of HA-1004.

Figure 8. Diamide-mediated pulmonary vasodilation is significantly inhibited by reducing transmembrane K⁺ gradient. *A:* Representative tracings showing 100 µM diamide-mediated tension changes in PA rings constricted by 25 mM K⁺ (25K, left panel) and 80 mM K⁺ (80K, right panel). *B:* Summarized data (means±SE) showing the amplitude of 25K- (left panel; n=4) and 80K- (right panel; n=5) mediated active tension before (control), during, and after (washout) extracellular application of 100 µM diamide. ** P<0.01 vs. control and washout. *C:* Summarized data (means±SE) showing the amplitude of active tension induced by raising extracellular K⁺ from 4.7 to 20, 25, 30, 35, 40, and 80 mM (open circles; n=4-8), respectively, and the percentage reduction of corresponding active tension induced by 100 µM diamide (closed circles; n=4-8).

Figure 9. Diamide-mediated pulmonary vasodilation is not significantly changed in PA rings constricted with different concentrations of phenylephrine (PE). *A:* Representative tracings showing 100 µM diamide-mediated tension changes in PA rings constricted by 0.03 µM PE (left panel) and 100 µM PE (right panel). *B:* Summarized data (means±SE) showing the amplitude of 0.03 µM PE- (left panel; n=4) and 100 µM PE (right panel; n=6)-mediated active tension before (control), during, and after (washout) extracellular application of 100 µM diamide. ** P<0.01 vs. control and washout. *C:* Summarized data (means±SE) showing the amplitude of active tension induced by 0.01, 0.03, 0.1, 1, 10 and 100 µM PE (open circles; n=4-7), respectively, and the percentage reduction of corresponding active tension induced by 100 µM diamide (closed circles; n=4-9).

Figure 10. Pulmonary vasodilation induced by the K⁺ channel opener cromakalim is abolished by reducing transmembrane K⁺ gradient. *A:* Representative tracings showing 1 μM cromakalim-mediated tension changes in PA rings constricted by 25 mM K⁺ (25K, left panel) and 80 mM K⁺ (80K, right panel). *B:* Summarized data (means±SE) showing the amplitude of 25K- (left panel; n=6) and 80K- (right panel; n=6) mediated active tension before (control), during, and after (washout) extracellular application of cromakalim. *** P<0.001 vs. control and washout.

Figure 11. Thiol oxidants increase whole-cell K⁺ currents. *A:* A representative record of outward K⁺ current (*a*), elicited by a test potential of +60 mV (holding potential, -70 mV), before (Control) and after (Diamide) extracellular application of 100 μM diamide in a rat PASMC. Summarized data (means±SE; n=9 cells, *b*) showing the amplitudes of the transient (I_{Tr}) and steady-state (I_{ss}) components of the currents at +60 mV in PASMC before (Control, gray bars) and after (solid bars) application of diamide. ** P<0.01 vs. Control. *B:* Representative currents (*a*), elicited by a series of test potentials ranging from -60 to +80 mV in 20-mV increments (holding potential, -70 mV), before (Control) and during extracellular application of hydrogen peroxide (H₂O₂, 50 μM) in the presence (H₂O₂+4-AP) or absence (H₂O₂) of 4-aminopyridine (4-AP, 5 mM) in a H9c2 cell. Summarized data (means±SE; n=7 cells, *b*) showing the current-voltage (I-V) relationship curves in H9c2 cells before (Control, open circles) and during exposure to H₂O₂ (closed circles) or H₂O₂+4-AP (gray triangles).

Figure 12. Effect of functional removal of endothelium on diamide-mediated pulmonary vasodilation. *A:* Representative tracings showing active tension induced by 25 mM K⁺ (25K) in the presence or absence of 10 μM acetylcholine (ACh) or 100 μM diamide in PA rings with

intact (+*Endo*, upper panel)) and denuded (-*Endo*, lower panel) endothelium. Note that ACh-mediated vasodilation is abolished in the endothelium-denuded (-*Endo*, lower panel) PA ring. *B*: Time course of the decline phase of diamide-mediated relaxation, corresponding to the shadowed areas in *A*, in PA rings with (+*Endo*) or without (-*Endo*) endothelium. *C*: Summarized data (means±SE; n=8) showing amplitude of PE-induced active tension before (control), during, and after (washout) application of 100 μM diamide in PA rings with (+*Endo*) and without (-*Endo*) endothelium. *** P<0.001 vs. control and washout.

Figure 13. Diamide inhibits CCE-mediated PA contraction induced by active store depletion. *A*: Representative tracings showing active tension induced by PE-mediated Ca²⁺ release (in the absence of extracellular Ca²⁺) and by store depletion-mediated Ca²⁺ influx or capacitive Ca²⁺ entry (CCE, in the presence of Ca²⁺ and 1 μM phentolamine) under control condition (*a*) and during the treatment with 100 μM diamide (which was applied to the vessels with phentolamine, *b*). *B*: Summarized data (means±SE; n=12) showing PE-mediated transient PA contraction in the absence of extracellular Ca²⁺ (*a*) when the vessels were first challenged with PE (1st, grey bar) and challenged with PE after ~15 min (2nd, solid bar), and CCE-induced PA contraction in vessels treated with (*Diamide*) or without (*Control*) 100 μM diamide. *** P<0.001 vs. Control.

Figure 14. CCE-induced PA contraction is similarly preserved with successive challenges. *A*: Representative tracings showing active tension induced by store depletion-mediated Ca²⁺ influx or capacitive Ca²⁺ entry (CCE; see Fig. 13 legend for details). The store depletion was induced by two successive PE challenges in the presence of 1 μM phentolamine; the 2nd challenge was given approximately 90 min after the first challenge. *B*: Summarized data (means±SE; n=8)

showing the amplitude of CCE-induced PA contraction when the vessels were first challenged with PE (*1st*, gray bar) and challenged with PE after 90 min (*2nd*, solid bar). * $P<0.05$ vs. gray bar.

Figure 15. Diamide inhibits CCE-mediated PA contraction induced by passive store depletion. *A*: Representative tracings showing active tension induced by 40 mM K⁺ (40K, left panels) and by store depletion-mediated Ca²⁺ influx or capacitive Ca²⁺ entry (CCE) as a result of CPA (50 μM)-mediated passive depletion of intracellular stores in control PA rings (upper panels) and 100 μM diamide-treated PA rings (lower panels). *B*: Summarized data (means±SE; n=8) showing amplitude of 40K-mediated active tension [*a*, when the vessels were first challenged (*1st*) and challenged 15 min later (*2nd*)] in PA rings without treatment of diamide, and CPA-induced PA contraction due to CCE (*b*) in control (grey bars) and diamide-treated (solid bars) PA rings. The CCE-induced active tension was normalized to the 40K-mediated active tension and expressed as percentage of corresponding 40K-mediated contraction. ** $P<0.01$ vs. control.

Figure 16. Increase of extracellular [K⁺] to 80 mM abolished diamide-mediated pulmonary vasodilation. *A*: Representative tracings showing active tension induced by 80 mM K⁺ (80K) before, during, and after application of 300 μM diamide (left panel), as well as before and during application of 0.1 μM nifedipine (right panel). *B*: Summarized data (means±SE; n=4) showing tension before (basal) and during application of 80K in the presence (80K+diamide) or absence (80K) of diamide (300 μM). *C*: Summarized data (means±SE; n=4) showing tension before (basal) and during application of 80K in the presence (80K+nif) or absence (80K) of nifedipine (Nif, 0.1 μM). *** $P<0.001$ vs. 80K.

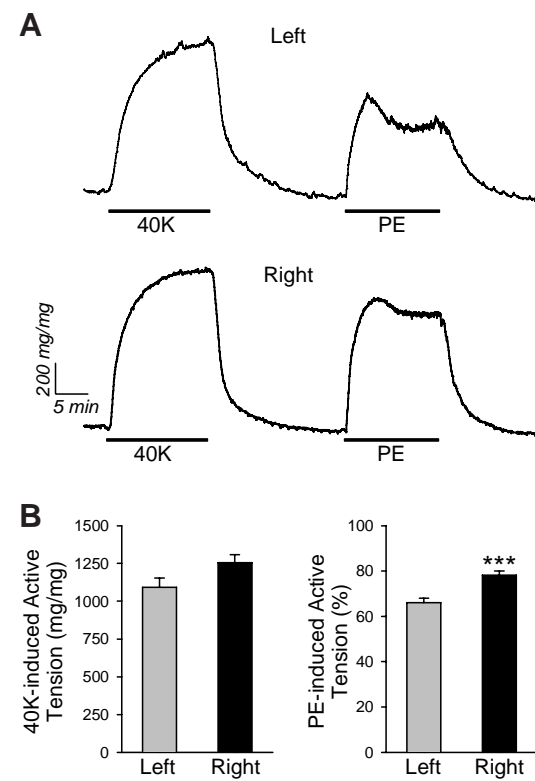


Fig. 1

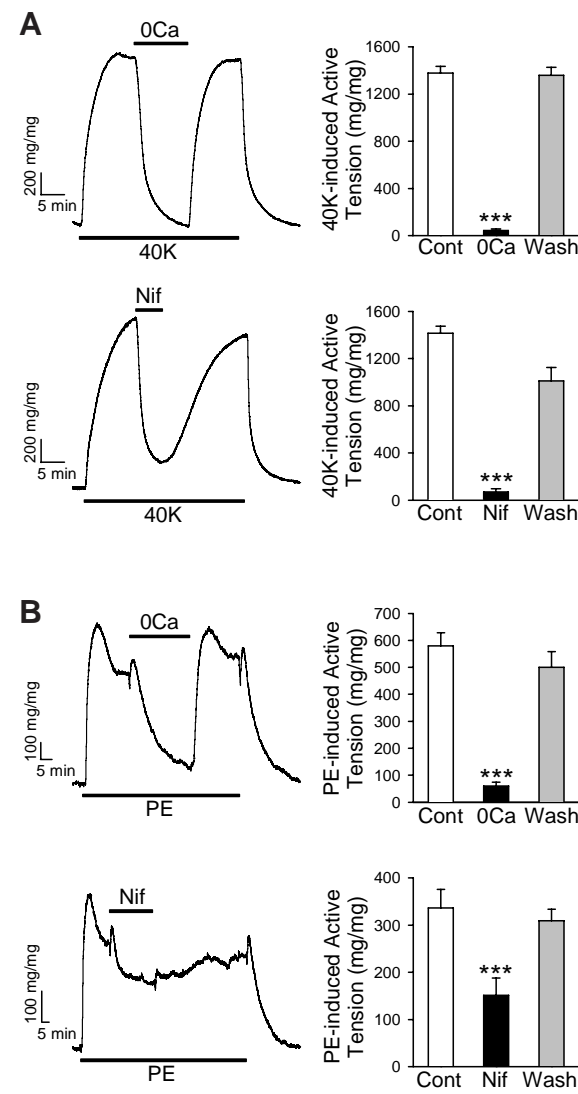


Fig. 2

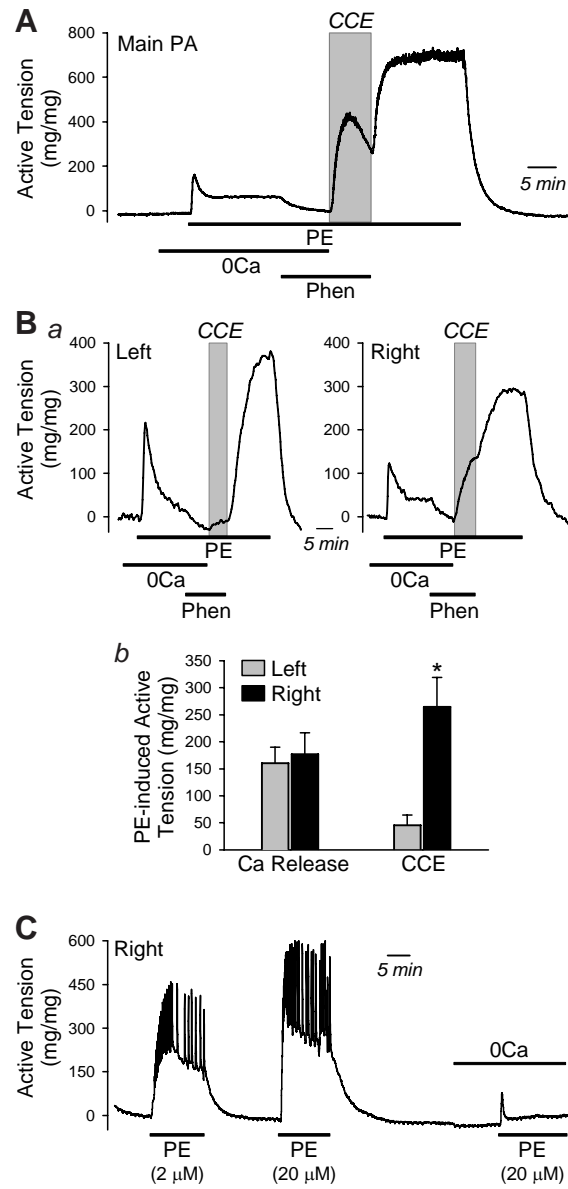


Fig. 3

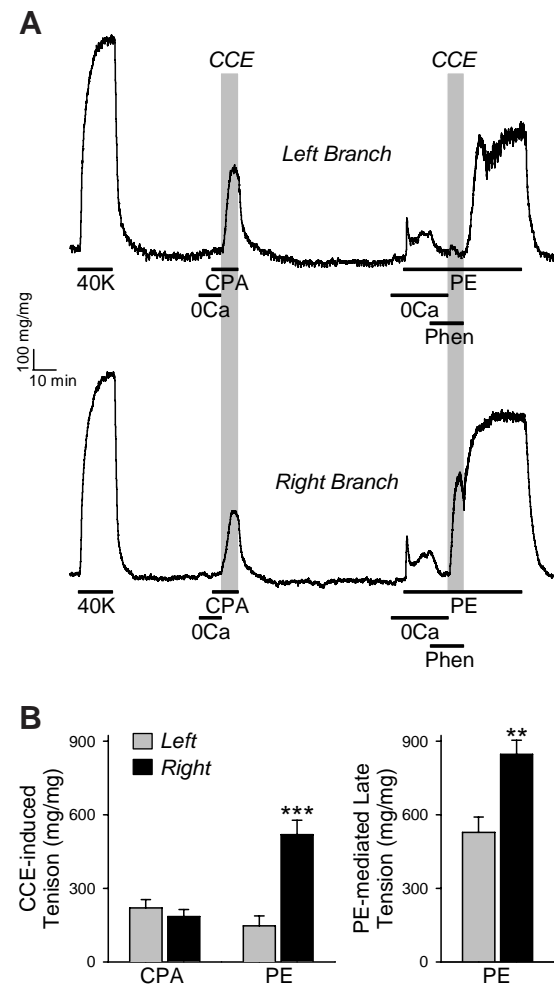


Fig. 4

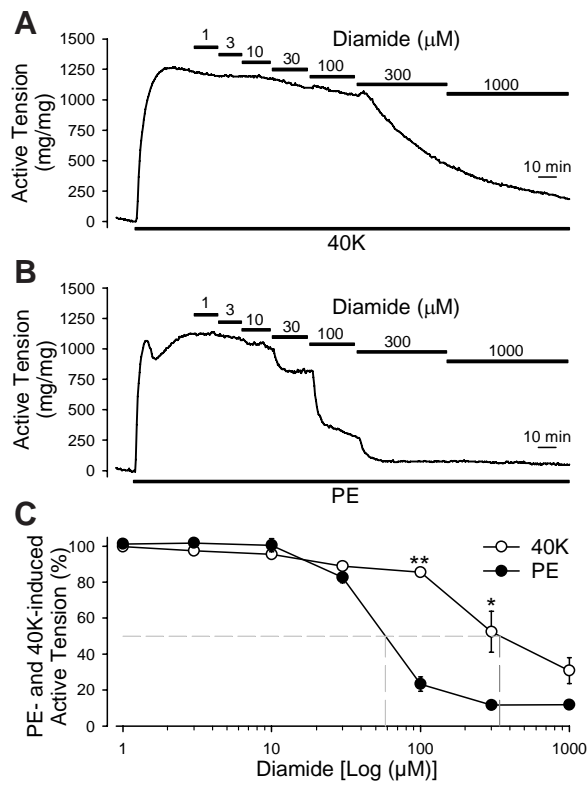


Fig. 5

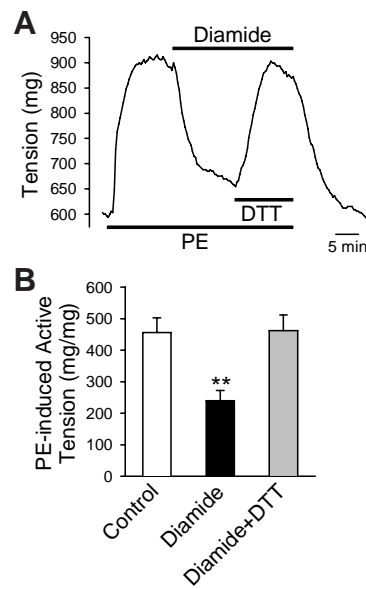


Fig. 6

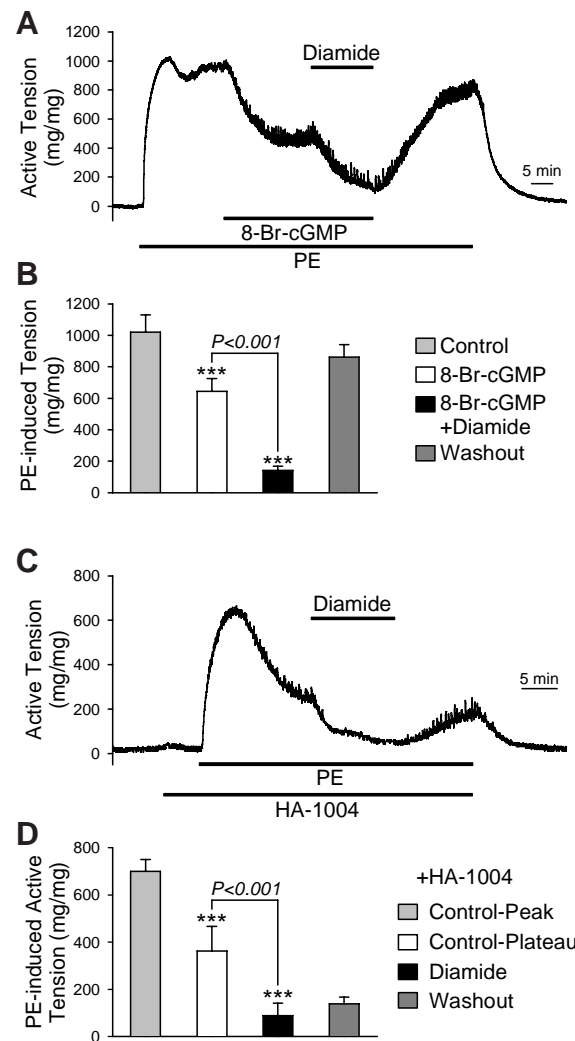


Fig. 7

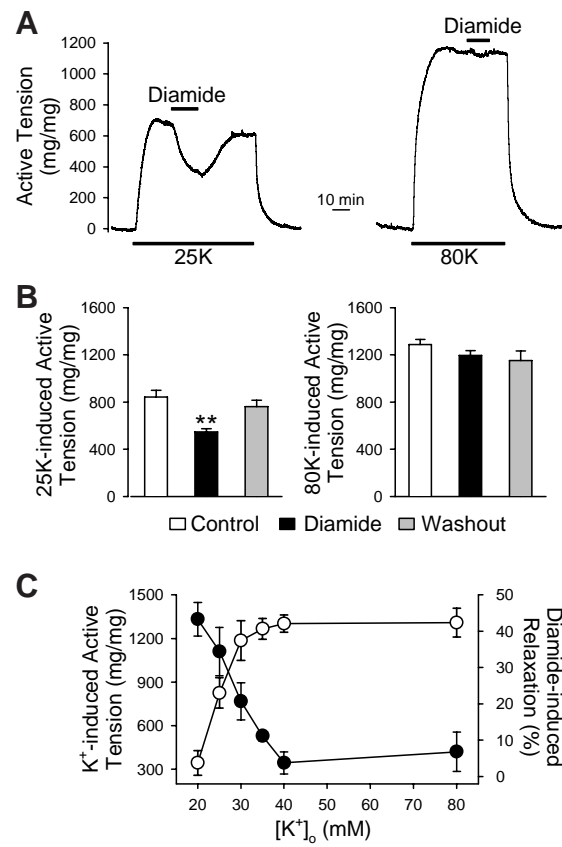


Fig. 8

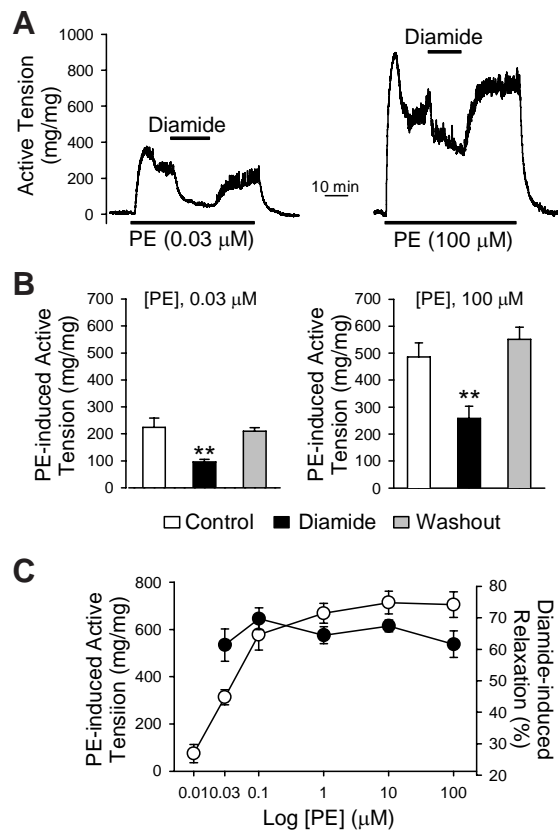


Fig. 9

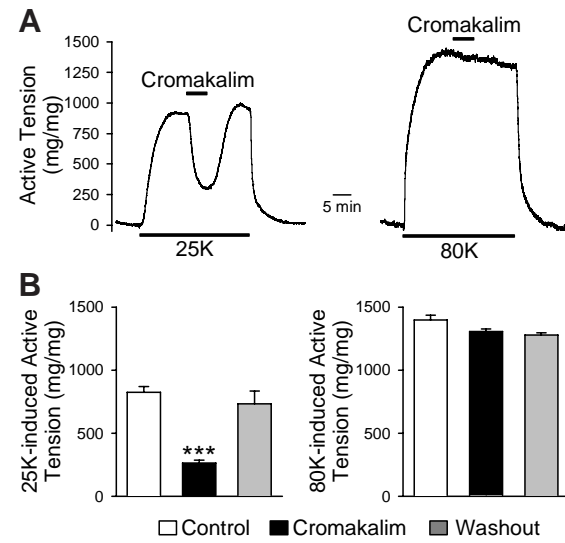


Fig. 10

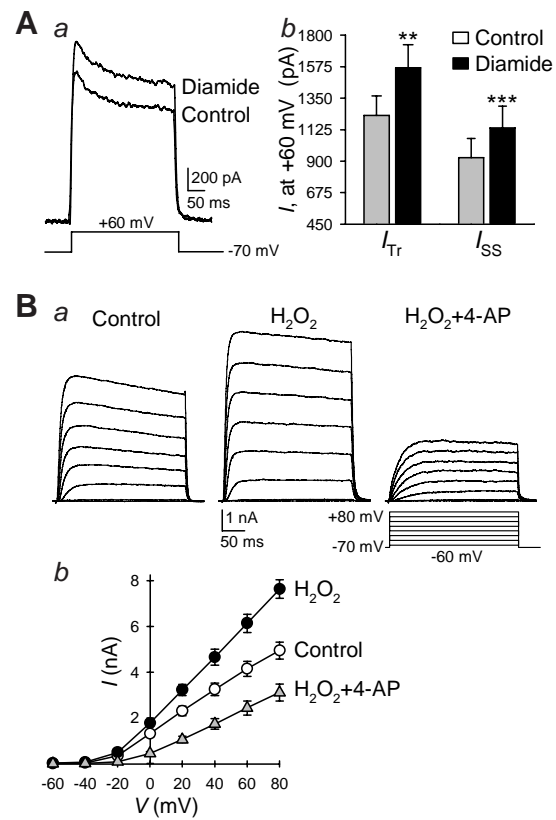


Fig. 11

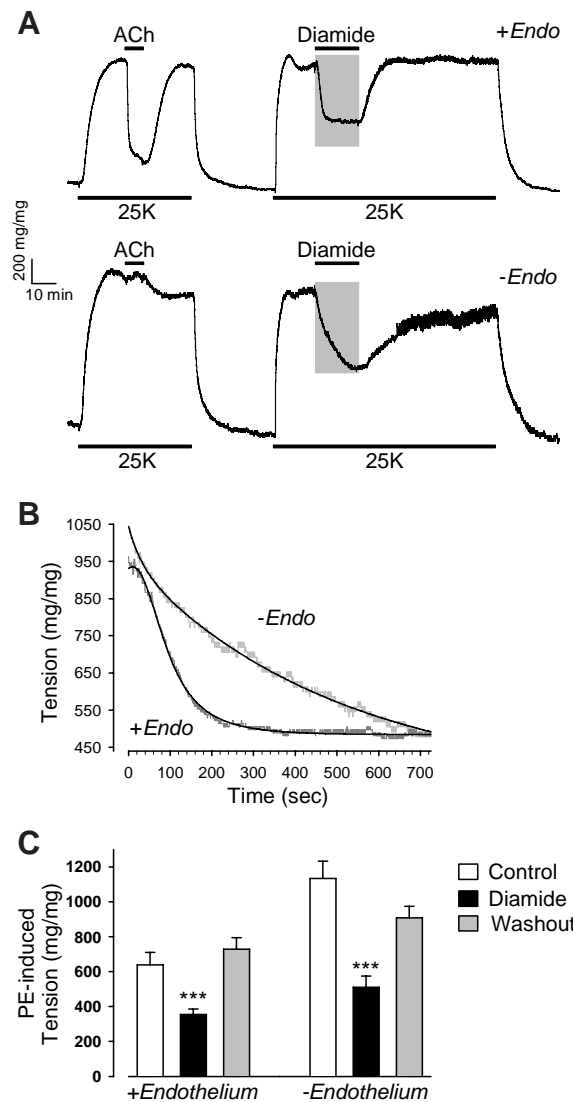


Fig. 12

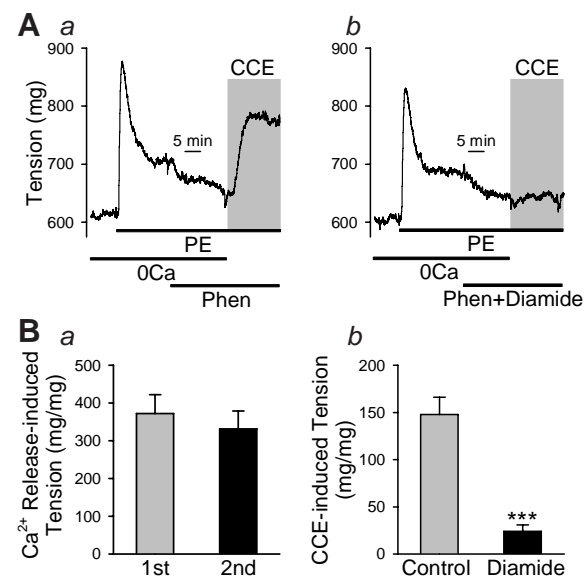


Fig. 13

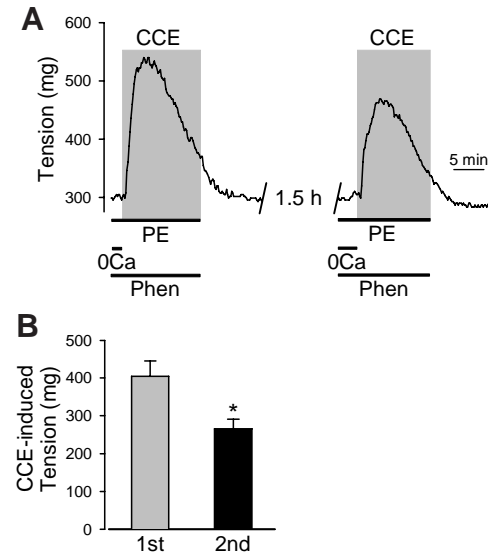


Fig. 14

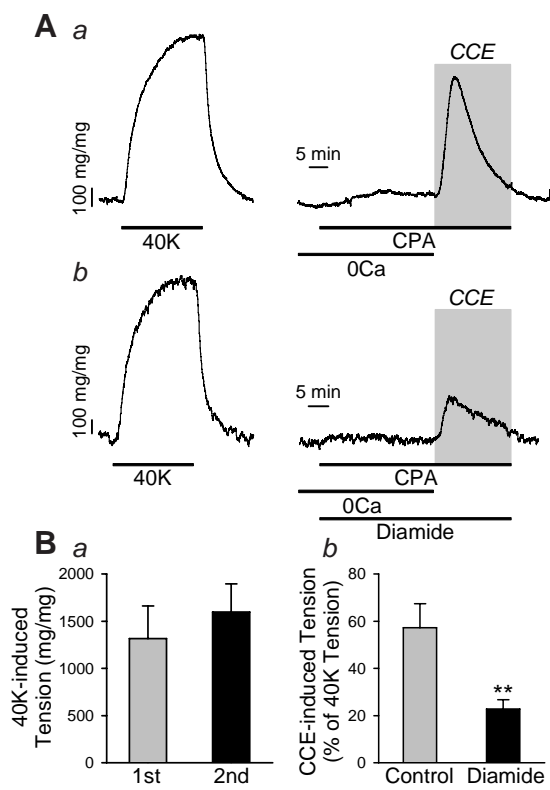


Fig. 15

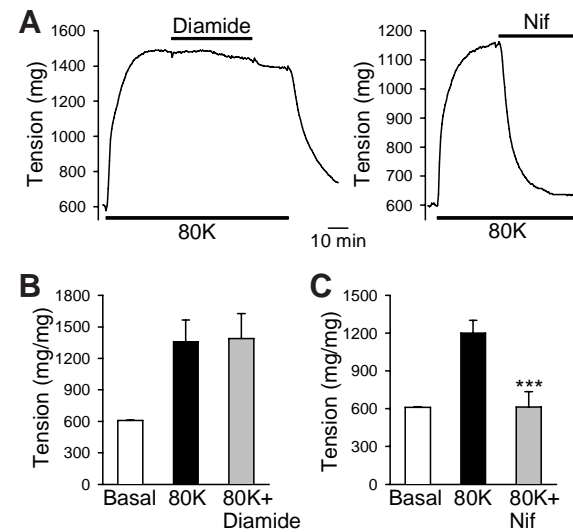


Fig. 16